Available online at www.sciencedirect.com
SCIENCE DIRECT
Scripta Materialia 54 (2006) 381–386
Scripta MATERIALIA
www.actamat-journals.com

Does metallic glass have a backbone? The role of percolating short range order in strength and failure

Y. Shi, M.L. Falk *

Materials Science and Engineering, University of Michigan, 2300 Hayward Street, Ann Arbor, MI 48109 2136, United States

Received 6 April 2005; received in revised form 23 May 2005; accepted 30 September 2005
Available online 2 November 2005

Abstract

Simulation studies indicate that metallic glasses derive their exceptional strength from a percolating backbone of short range order. The percolation of this structure coincides with a high stresses prior to yield and the development of strain localization. Examples are presented from two- and three-dimensional molecular dynamics investigations.

Keywords: Shear bands; Metallic glasses; Molecular dynamics; Simulation; Mechanical properties

1. Introduction and background

Recent advances have brought the development of bulk metallic glass (BMG) as a high strength, failure resistant structural material significantly closer to realization. The primary obstacle to the use of BMG in structural applications has long been the lack of hardening which, at temperatures significantly below the glass temperature, leads to dramatic failure modes associated with strain localization [1–4]. Initial attempts to overcome this limitation concentrated on the use of embedded crystalline phases to interfere with the propagation of shear bands [2,5,6]. However, recent studies have revealed that monolithic BMG can also exhibit exceptionally high ductility potentially equal to or exceeding that of such complex nanocomposites [7,8]. These developments illustrate quite dramatically that there exist important aspects of glass structure that, if properly understood, could guide the development of a new class of practical structural alloys.

A good deal of research has focused on the question of how to design alloys which are good glass formers [1,9]. Considerably less attention has been paid to the relationship between structure and mechanical properties. However, a number of recent observations regarding glass structure provide tantalizing clues as to what aspects of structure may play an important role in both of these properties. An icosahedral phase has been observed to precipitate in some zirconium based glasses and exists in the as-quenched glass on a nanometer scale possibly stabilizing the glassy state [10,11]. A glass phase has been observed in pure zirconium at high pressures and temperatures that, once formed, is unusually stable [12]. Recently microstructural data has been interpreted to infer that a glass phase can precipitate from the melt in an aluminum based glass [13]. Each of these observations points to the critical role played by energetically favorable aperiodic short range order in stabilizing the glass. The last observation, if borne out, indicates that such short range ordering might result in a distinct low-energy glass phase.

Regardless of whether the short range ordering responsible for stable glass formation is icosahedral in nature or a more complex association related to cluster packing, as has been recently suggested [9], the consequences of short range order on mechanical properties are dramatic. We have performed simulations of systems with differing degrees of short range order produced by quenching from the liquid

* Corresponding author. Tel.: +1 734 615 8086; fax: +1 734 763 4788.
E-mail address: mfalk@umich.edu (M.L. Falk).

1359-6462/$ - see front matter
doi:10.1016/j.scriptamat.2005.09.053

at different rates. In each case we can quantify the degree of short range order that develops in the glass and the resulting mechanical response. In all cases the glasses with more short range order exhibit higher strength coupled with a stronger propensity toward localized deformation. We are able to show directly that the localization phenomenon corresponds to the breakdown of the short range ordering in the glass. Additionally, careful analysis of the strain rate dependence of the localization shows that the cross-over from homogeneous to localized flow corresponds to a percolation transition in the underlying short range ordering. This result is potentially important for predicting the structural conditions for localization in metallic glass.

2. Simulation methodology

We have performed molecular dynamics simulation on a number of different systems. The two we will discuss here are a two-dimensional binary alloy and a three-dimensional single-component system. Both systems were designed such that the underlying bonding conspires to raise the energetic cost of states with periodic long-range order relative to aperiodic short-range ordered states.

The binary alloy is composed of two species that we will refer to as S and L for small and large, interacting via a Lennard-Jones potential of the form [14,15]

$$U_{\alpha\beta}(r) = 4\varepsilon_{\alpha\beta}\left[\left(\frac{\sigma_{\alpha\beta}}{r}\right)^{12} - \left(\frac{\sigma_{\alpha\beta}}{r}\right)^{6}\right], \tag{1}$$

where, between an atom of species α and an atom of species β, $\varepsilon_{\alpha\beta}$ represents the energy of the bond and $\sigma_{\alpha\beta}$ provides a length scale, the distance at which the interaction energy is zero. The SS and LL bond energies are half that of the SL bond energy, $\varepsilon_{SS} = \varepsilon_{LL} = \frac{1}{2}\varepsilon_{SL}$. The SS and LL length scales are related to the SL length scale as

$$\sigma_{SS} = 2\sigma_{SL}\sin\left(\frac{\pi}{10}\right), \qquad \sigma_{LL} = 2\sigma_{SL}\sin\left(\frac{\pi}{5}\right). \tag{2}$$

In this binary system we will take the reference length scale to be σ_{SL} and the reference energy scale to be ε_{SL}. All the particles will have the same mass, m_0, which will be the reference mass scale. The reference time scale t_0 will therefore be $\sigma_{SL}\sqrt{m_0/\varepsilon_{SL}}$. In order to make rough comparisons to experiments and to present times in physical units we will consider that for a typical material $t_0 \approx 1$ ps, and $\sigma_{SL} \approx 3$ Å. Interactions were neglected beyond a cutoff distance that corresponded to $U_{\alpha\beta}(r_{c,\alpha\beta}) = 0.0163\varepsilon_{SL}$. For interactions between S atom and L atom, the cutoff $r_{c,SL}$ is therefore $2.5\sigma_{SL}$.

This system exhibits both crystalline and quasi-crystalline ground states [15,16]. Perhaps because the crystalline unit cell is quite large and the quasi-crystalline state is close in energy, this system exhibits a strong tendency toward amorphization, while many other two-dimensional systems show a strong tendency to crystallize. It has been used extensively to study quasi-crystal and amorphous thermodynamic and mechanical properties [14,16–18,34]. We chose our composition $N_L : N_S = (1+\sqrt{5}) : 4$ to be consistent with other studies of this system. T_{MCT}, the mode coupling temperature, was measured to be $0.325\varepsilon_{SL}/k$, where k is the Boltzmann factor. For the sake of comparison temperatures will be measured in units of T_{MCT}.

The three-dimensional single-component system simulated is a Dzugutov glass where interactions between atoms are described by the potential

$$U(r) = A(r^{-m} + B)\exp\left(\frac{c}{r-a}\right)\Theta(a-r) + B\exp\left(\frac{d}{r-b}\right)\Theta(b-r). \tag{3}$$

The parameters m, A, B, a, b, c and d are chosen as described in Ref. [19] and Θ represents the Heaviside step function which enforces the short range nature of each of the terms. This potential is chosen to have a maximum near the distance at which neighboring atoms would necessarily reside in order to form a face-centered cubic, body-centered cubic or hexagonal close-packed crystal. Since crystallization is frustrated in this way, the Dzugutov system is a glass former. It has been observed that icosahedral order plays a significant role in the onset of supercooled liquid behavior in this system [20,21]. All quantities are measured in reduced units: σ (length scale), t_0 (time scale) and ε (energy scale) [19]. The mode coupling temperature of this system $T_{MCT} = 0.4$ [20].

The strain rates accessible to molecular dynamics are high, approximately 10^6–10^9 s^{-1} in this study. To overcome this limitation we simulated over several orders of magnitude in strain rate to extrapolate to the quasi-static regime. This extrapolation omits the effect of creep that necessarily involves complex thermally activated events.

3. Simulation results

3.1. Two-dimensional nanoindentation studies

The initial conditions for the nanoindentation studies were created from the two-dimensional binary alloy system described above by starting from supercooled liquids equilibrated above T_{MCT}. Subsequent to equilibration the temperature of the liquid was reduced to 9.2% of T_{MCT}. Two samples were created. Sample (a) was cooled at a rate of $0.98\times10^{-4}T_{MCT}/t_0$, corresponding to a quench over approximately 10 ns, and sample (b) was cooled at a rate of $1.97\times10^{-6}T_{MCT}/t_0$, corresponding to a quench over approximately 0.5 μs. Then each sample was tiled 5 across by 2 down to create a single slab of 200,000 atoms which formed the $285\sigma_{SL}$ or approximately 87 nm thick film. The indenter is a semi-circle of atoms extracted from the amorphous sample. The positions of the indenter atoms are fixed except for rigid movement during indentation. Therefore this indenter adheres to the surface and the indentation is significantly non-Hertzian. Other simulations were performed with a frictionless Hertzian indenter, and these results have been published elsewhere [18]. The

indenter radius was chosen to be $250\sigma_{SL}$, approximately 75 nm. The boundary conditions constrain the film in the in-plane direction, perpendicular to the indenter loading direction, while maintaining periodic boundary condition (PBC). The underside of the film is held fixed as if the amorphous film were deposited upon a substrate of infinite stiffness. The indenter is lowered into the sample film under displacement control at a velocity $0.001\sigma_{SL}/t_0$, or approximately 0.3 m/s. During nanoindentation, the temperature of the whole system is maintained at 9.2% T_{MCT} by coupling to a Nose–Hoover thermostat [22–24].

Fig. 1 shows the results of each of these simulations. The top image in each case show the deviatoric shear strain distribution calculated by a least-mean-square fitting procedure [17]. Shear localization underneath the indenter reminiscent of experimental observations are evident in (b) [25]. The bottom image shows a structural analysis of the final configuration. This analysis utilizes the fact that this system has an underlying quasi-crystalline ground state [14]. The quasi-crystal of this system is composed of nine distinct atomic motifs consisting of an atom and its nearest neighbors. We have analyzed the structure of the samples, and we have determined if each atom exhibits such quasi-crystal-like short range order. In the bottom images of Fig. 1, darker regions have a lower percentage of such short range order, and lighter regions have more atoms in these configurations. Before indentation (a) has 58% of its atoms in stable motifs; sample (b) has 74% in stable motifs. During indentation the number of atoms in stable motifs decreases in both samples. It is apparent in Fig. 1 that in sample (b) the shear bands coincide with regions in which atoms are no longer in stable motifs. In sample (a) no such change is evident under the indenter.

3.2. Two-dimensional uniaxial tensile tests

In order to understand why dramatic localization is evident in sample (b) and not in sample (a) we also performed a large number of smaller simulations of uniaxial tensile loading on the samples produced from the same two-dimensional binary alloy [33]. The initial conditions were created by equilibrating the 20,000-particle system as a pressurized liquid and reducing the temperature to 9.2% of T_{MCT} by cooling at constant volume. The most gradually quenched sample was cooled at an effective rate of $9.85\times10^{-7}T_{MCT}/t_0$ corresponding to a quench over approximately 1 μs. Other samples were quenched at rates as much as 1000 times higher. In addition a number of samples were produced by quenching instantaneously from melts of different temperatures by rescaling the particle velocities and then allowing the system to age for $100t_0$, approximately 0.1 ns. The residual pressure was released by uniformly expanding the sample at a strain rate $10^{-6}t_0^{-1}$. Free surfaces were then introduced by eliminating periodicity along the surfaces parallel to the y-axis followed by a relaxation for $10{,}000t_0$, approximately 10 ns. In each case we characterize the structure of the resulting material by the potential energy per atom of the sample prior to the mechanical test. A systematic decrease of the Poisson ratio was observed with decreasing quench rate. Six (for instantaneously quenched samples) or 10 (for slowly quenched samples) independent samples were created following each quenching schedule to determine the effects of sample to sample variation.

In order to quantify the degree of localization we define a quantity that we will call the deformation participation ratio (DPR). The DPR is the fraction of atoms that in their vicinity undergo a local deviatoric shear strain larger than the nominal deviatoric shear strain of the entire sample. The deviatoric shear strain is extracted from the atomic positions using the procedure for extracting a best fit strain [17]. In a homogeneously deforming sample the DPR should be approximately 0.5. However, during a highly localized deformation the DPR should become negligible, approaching the ratio of the shear band width to the system size. Fig. 2(a) shows the DPR at 5% strain as a function of strain rate for different quenching schedules on a log–log scale. Each line in Fig. 2(a) corresponds to a different quenching schedule that can be characterized by a

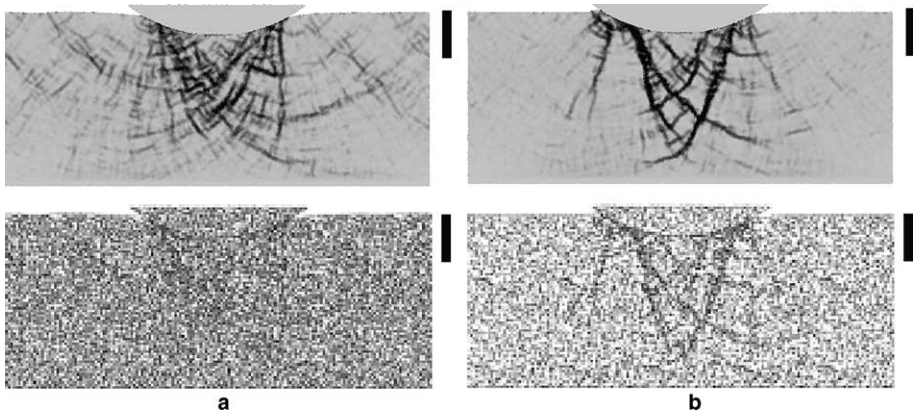

Fig. 1. Two simulations of nanoindentation in a two-dimensional binary glass. Sample (b) was quenched over a period 50 times longer than sample (a). The top images show the degree of local deviatoric strain underneath the indenter. Sample (b) shows much more dramatic localization underneath the indenter. The bottom images are lighter where there exists a high degree of quasi-crystal-like short range order. The breakdown of such ordering is evident in sample (b). The scale bar represents $80\sigma_{SL}$ or 24 nm.

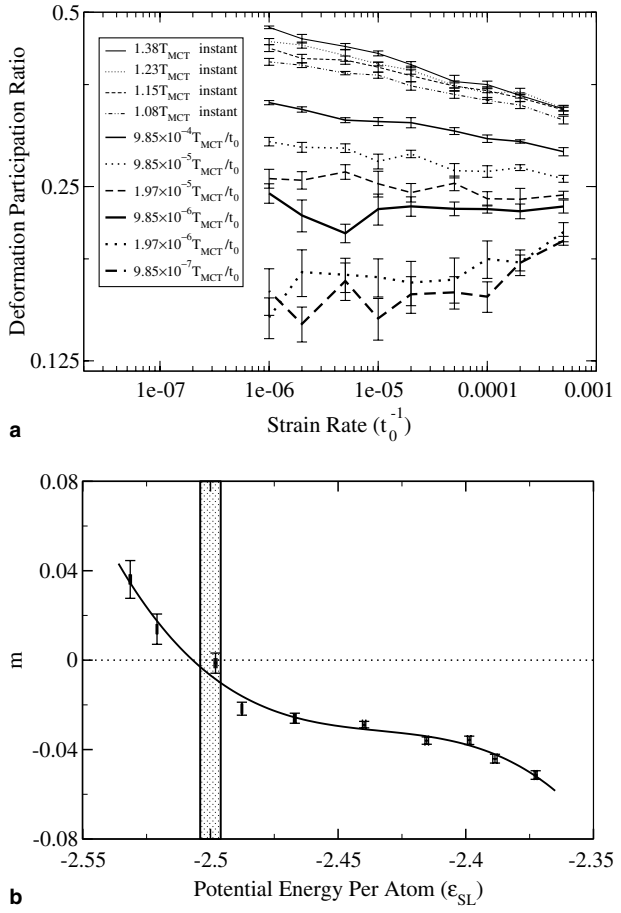

Fig. 2. Graph (a) shows the deformation participation ratio, the fraction of atoms with local strain higher than the nominal strain, as a function of strain rate. Each line represents a different quenching schedule and, hence, a different initial potential energy per atom. The quenching rates are shown in the legend. The strain rate sensitivity of the DPR, m, found by measuring the slopes of these curves in (a) are shown in (b) as a function of the potential energy per atom prior to the mechanical test. The cross-over from negative to positive slope corresponds closely to the existence of a percolating k-core cluster of quasi-crystal-like short range order prior to mechanical testing as represented by the vertical band in (b).

particular initial potential energy per atom. Fig. 2(b) shows the slope of each line in Fig. 2(a) as a function of this potential energy per atom. We will refer to this slope m as the strain rate sensitivity of the DPR. Note that this quantity exhibits a change in sign; the more gradually quenched glasses have positive strain rate sensitivities and the more quickly quenched glasses have negative strain rate sensitivities. This change in sign corresponds to a change in the limiting value of DPR in the quasi-static, i.e. low strain rate, limit. In the low strain rate limit glasses quenched gradually approach zero DPR and exhibit localization, while glasses quenched quickly approach the maximum allowed value of 0.5 DPR and exhibit homogeneous flow. As in recent work by Schroers and Johnson [8] less dramatic localization and higher apparent ductility occurred in samples with higher Poisson ratio.

We analyzed each of these samples prior to deformation to determine if the previously discussed quasi-crystal-like short range order percolated across the sample. This was done using both bond percolation and also k-core percolation in which each atom in the cluster must have at least $d+1=3$ neighbors also in the cluster, where $d=2$ is the dimensionality [26]. The band in Fig. 2(b) shows that a percolating k-core cluster is observed to occur at $-2.500 \pm 0.004\varepsilon_{SL}$. This coincides closely with the potential energy per atom at which m changes sign.

3.3. Three-dimensional uniaxial compression tests

In order to test whether this correspondence between percolation and mechanical behavior is limited to the two-dimensional models or this particular binary system we have performed uniaxial compression simulations in the three-dimensional single-component Dzugutov system. No shear band forms in uniaxial tension in this system due to the initiation of fracture. In this simulation we used a system containing 112,000 atoms at number density 0.84. The dimensions of the system are $74\sigma \times 114\sigma \times 16\sigma$. We quench the system from high temperature $2.5T_{MCT}$ to $0.075T_{MCT}$ and from a pressure from 6.0 to $0.0\varepsilon/\sigma^3$ over a period of $10{,}000t_0$ or $1000t_0$ through a constant temperature gradient and constant pressure gradient NPT simulation. Uniaxial compression is applied in y-direction where PBC is maintained. During compression the x-boundaries are free surfaces while z-boundaries are periodic and coupled to a barostat to preserve average stress σ_{zz} zero [27,28]. As shown in Fig. 3(a) the slowly quenched system exhibits pronounced localization in uniaxial compression when tested at a strain rate of $0.0001t_0^{-1}$. The systems quenched over one tenth of this time exhibit no significant localization. A structural analysis of the location of atoms with local icosahedral order is also shown in Fig. 3(b). The icosahedral centers are determined according to the criteria described in Ref. [19]. It is apparent that the region of localization corresponds to a breakdown in local icosahedral short range order.

We analyzed these two simulated systems to determine if the short range order percolated prior to mechanical testing. To do this we follow the example of Ref. [20] and perform a steepest descent energy minimization prior to structurally analyzing the system. We consider that if two icosahedra share at least three common neighbor atoms they constitute a mechanically stable link. By this definition the slower quenched sample shown in Fig. 3 contains a percolating backbone of short range order prior to mechanical testing, while the quickly quenched sample not shown does not exhibit such percolation. We anticipate undertaking a more thorough strain rate analysis similar to that performed on the two-dimensional system to see if the percolation transition again corresponds with the transition to localized deformation.

4. Discussion

It has long been appreciated that structural softening is the likely mechanism for shear localization [29]. Typically

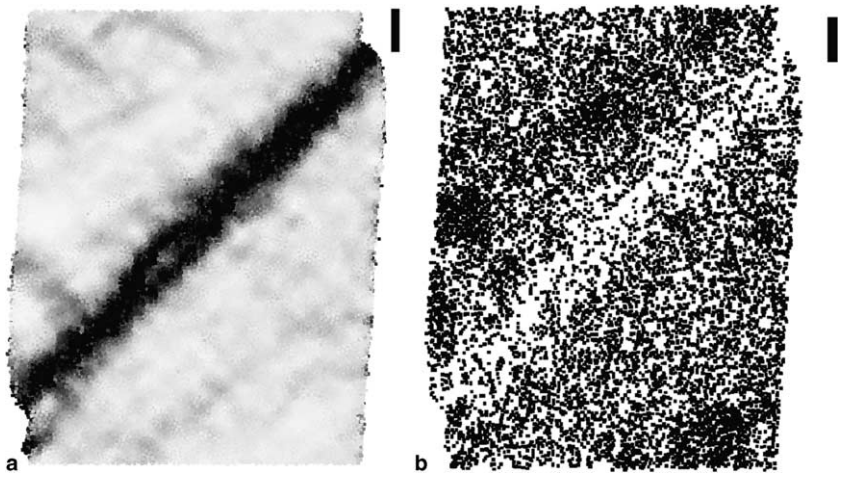

Fig. 3. The results of a single-component three-dimensional Dzugutov glass at 10% strain in uniaxial compression (both for the more slowly quenched sample): (a) areas of high deviatoric strain revealing evidence of localization, and (b) the location of centers of icosahedral order. The region of low icosahedral order on the right corresponds closely to the region of large strain on the left. The scale bar represents 10σ.

this phenomenon is described in terms of the generation of free volume in the material due to the application of shear. While we have observed increases in volume during shear in related simulation studies [30] inherent density fluctuations in the glass, particularly in multicomponent systems, make it exceedingly difficult to statistically resolve such changes on the scale of shear bands which are only nanometers in width.

Perhaps more importantly analysis in terms of free volume does not provide much insight that can be used to differentiate one glass from another. In glasses which develop multiple localized bands on intermediate scales [7,8] we would like to understand the aspects of the material structure that sets a typical shear band persistence length during deformation. Percolation of short range order provides one possible theoretical path to analyzing such materials. For example in certain glass systems introduction of a particular solute species may systematically frustrate the formation of a percolating backbone of short range order. The length scale of such frustration would, in such a case, be set by the concentration of the solute. Sensitivity to the concentration of the solute could be dramatic due to the nature of percolation as a phase transition that can have mixed discontinuous and continuous character [31]. In Hertzian sphere systems typically used to study granular matter diverging length scales have been measured in simulations approaching the transition both from below, associated with the number of interacting particles [32], and from above, associated with the vibrational density of states [33]. Connecting the glass mechanical behavior in failure to its structure could provide means to extract important information from careful analysis of changes in elastic properties and from neutron scattering data.

5. Conclusions

Simulations of two- and three-dimensional glass systems under nanoindentation and uniaxial tension reveal that strain localization is associated with the breakdown of local short range order. In the two-dimensional binary alloy a transition is observed in the strain rate dependence of the degree of localization. This implies a cross-over between homogeneous flow and inhomogeneous flow in the quasi-static limit as a function of the degree of glass relaxation. This transition coincides with the percolation of atoms exhibiting short range order in the glass. The results are substantiated by simulations of uniaxial compression behavior in a single-component three-dimensional glass.

Acknowledgements

The authors would like to acknowledge the support of the US National Science Foundation under Grant DMR-0135009. We are also grateful to the University of Michigan Center for Advanced Computing.

References

[1] Johnson WL. MRS Bull 1999;24:42.
[2] Hays CC, Kim CP, Johnson WL. Phys Rev Lett 2000;84:2901.
[3] Fan C, Li CF, Inoue A, Haas V. Phys Rev B 2000;61:R3761.
[4] Hufnagel TC, El-Deiry P, Vinci RP. Scr Mater 2000;43:1071.
[5] Xing LQ, Herlach DM, Cornet M, Bertrand C, Dallas JP, Trichet MF, et al. Mater Sci Eng A—Struct 1997;226:874.
[6] Inoue A, Wang XM. Acta Mater 2000;48:1383.
[7] Das J, Tang MB, Kim KB, Theissmann R, Baier F, Wang WH, Eckert J. Phys Rev Lett 2005;94:205501.
[8] Schroers J, Johnson WL. Phys Rev Lett 2004;93.
[9] Miracle DB. Nature Mater 2004;3:697.
[10] Saida J, Kasai M, Matsubara E, Inoue A. Ann Chim—Sci Mater 2002;27:77.
[11] Saksl K, Franz H, Jovari P, Klementiev K, Welter E, Ehnes A, et al. Appl Phys Lett 2003;83:3924.
[12] Zhang JH, Zhao YS. Nature 2004;430:332.
[13] Cahn JW, Bendersky LA. Amorphous and Nanocrystalline Metals. In: Busch R et al., editors. MRS Symposium Proceedings No. 806. Pittsburgh: Materials Research Society; 2004. p. 139–43.

[14] Widom M, Strandburg KJ, Swendsen RH. Phys Rev Lett 1987;58:706.
[15] Lancon F, Billard L, Chaudhari P. Europhys Lett 1986;2:625.
[16] Lee HK, Swendsen RH, Widom M. Phys Rev B 2001;64:224201.
[17] Falk ML, Langer JS. Phys Rev E 1998;57:7192.
[18] Shi YF, Falk ML. Appl Phys Lett 2005;86:011914.
[19] Dzugutov M. Phys Rev A 1992;46:R2984.
[20] Zetterling FHM, Dzugutov M, Simdyankin SI. J Non-Cryst Solids 2001;293:39.
[21] Dzugutov M, Simdyankin SI, Zetterling FHM. Phys Rev Lett 2002;89.
[22] Hoover WG. Phys Rev A 1985;31:1695.
[23] Nose S. Mol Phys 1984;52:255.
[24] Nose S. J Chem Phys 1984;81:511.
[25] Ramamurty U, Jana S, Kawamura Y, Chattopadhyay K. Acta Mater 2005;53:705.
[26] Chalupa J, Leath PL, Reich GR. J Phys C: Solid State 1979;12:L31.
[27] Parrinello M, Rahman A. J Appl Phys 1981;52:7182.
[28] Parrinello M, Rahman A. J Chem Phys 1982;76:2662.
[29] Steif PS, Spaepen F, Hutchinson JW. Acta Metall Mater 1982;30:447.
[30] Albano F, Falk ML. J Chem Phys 2005;122:154508.
[31] Schwarz JM, Liu AJ, 2004. Available from: cond-mat/0410595.
[32] Drocco JA, Hastings MB, Reichhardt CJO, Reichhardt C, 2004. Available from: cond-mat/0310291.
[33] Silbert LE, Liu AJ, Nagel SR, 2005. Available from: cond-mat/0501616.
[34] Shi Y, Falk ML. Phys Rev Lett 2005;95:095502.